KURENAI

Kyoto University Research Information Repository

KYOTO UNIVERSITY

Title	Nonequilibrium Phase Transitions and a Nonequilibrium Critical Point from Anti-de Sitter Space and Conformal Field Theory Correspondence
Author(s)	Nakamura, Shin
Citation	Physical Review Letters (2012), 109(12)
Issue Date	2012-09-18
URL	http://hdl.handle.net/2433/160370
Right	© 2012 American Physical Society
Type	Journal Article
Textversion	publisher

Kyoto University

Nonequilibrium Phase Transitions and a Nonequilibrium Critical Point from Anti–de Sitter Space and Conformal Field Theory Correspondence

Shin Nakamura[*]

Department of Physics, Kyoto University, Kyoto 606-8502, Japan
(Received 9 May 2012; published 18 September 2012)

We find novel phase transitions and critical phenomena that occur only outside the linear-response regime of current-driven nonequilibrium states. We consider the strongly interacting $(3 + 1)$-dimensional $\mathcal{N} = 4$ large-N_c $SU(N_c)$ supersymmetric Yang-Mills theory with a single flavor of fundamental $\mathcal{N} = 2$ hypermultiplet as a microscopic theory. We compute its nonlinear nonballistic quark-charge conductivity by using the AdS/CFT correspondence. We find that the system exhibits a novel nonequilibrium first-order phase transition where the conductivity jumps and the sign of the differential conductivity flips at finite current density. A nonequilibrium critical point is discovered at the end point of the first-order regime. We propose a nonequilibrium steady-state analogue of thermodynamic potential in terms of the gravity-dual theory in order to define the transition point. Nonequilibrium analogues of critical exponents are proposed as well. The critical behavior of the conductivity is numerically confirmed on the basis of these proposals. The present work provides a new example of nonequilibrium phase transitions and nonequilibrium critical points.

Introduction.—Nonequilibrium physics is one of the central subjects in modern physics. Although the linear response theory gives the transport coefficients at the vicinity of thermal equilibrium, its extension to the nonlinear regime is still a great challenge. In this Letter, we apply the anti–de Sitter space (AdS)/conformal field theory (CFT) correspondence [1,2] to the study of nonequilibrium physics in the nonlinear regime. AdS/CFT correspondence is a map between a strongly interacting quantum gauge theory and a classical gravity. The map is essentially established at the level of microscopic theory. However, it also provides a new picture for statistical mechanics. The macroscopic physics, such as thermodynamics, of the gauge particles appears naturally in terms of the black hole physics on the gravity side [3].

Usually, a drawback of AdS/CFT is that we need to deal with an idealized gauge theory that is not exactly realized in nature at the microscopic level, in order to ensure that the correspondence is well defined. However, the aim of nonequilibrium statistical mechanics is to describe macroscopic properties common to a wide range of many-body systems regardless of the details of each microscopic theory. Our ultimate goal is to obtain new information on such macroscopic physics that is shared by the actual systems in nature. Phase transition and critical phenomena are ideal places to look for such information in light of their possible universality.

In this Letter, we study nonequilibrium phase transitions [4] by using the AdS/CFT correspondence. Our system consists of strongly interacting gauge-theory plasma driven to the nonequilibrium steady state (NESS) by a constant current. We discover novel nonequilibrium phase transitions and a nonequilibrium critical point in the nonlinear regime. We develop a formalism to analyze the nonequilibrium phase transitions as well: we propose NESS analogues of thermodynamic potential and critical exponents.

Our phase transitions are associated with the nonlinear conductivity of our system. It has been shown in Ref. [5] that the gauge-theory plasma, which will be defined in detail later, exhibits negative differential conductivity (NDC) in low current-density regions. This NDC is categorized as S-shaped NDC (SNDC) in Ref. [6]. Here, the differential conductivity is defined as $\partial J/\partial E$, where J and E are the current density and the external electric field acting on the charge carriers, respectively. The difference from the conventional conductivity $\sigma = J/E$ is that the differential conductivity here can be either negative or positive, whereas σ cannot be negative. In fact, SNDC has been experimentally observed in various current-driven systems [6], including in systems of strongly correlated electrons (for e.g., see Ref. [7]). It has been shown in Ref. [5] that the NDC is converted to positive differential conductivity (PDC) in high current-density regions. The transition from NDC to PDC was observed to be smooth in Ref. [5]: it is a crossover.

In this Letter, we discover first-order and second-order phase transitions between NDC and PDC. We also observe critical phenomena at the critical point. As far as the author knows, the current-driven nonequilibrium phase transitions between NDC and PDC, and the associated critical point, have been reported neither experimentally nor theoretically so far: the present work provides a new model of nonequilibrium phase transitions and nonequilibrium critical points.

Microscopic theory.—We choose our microscopic theory by asking how much of its AdS/CFT duality is

established, rather than asking whether the microscopic details are realized in nature, since we are interested in only the macroscopic properties of NESS that may be independent of the microscopic details. One of the gauge theories whose AdS/CFT duality is well established is the $(3 + 1)$-dimensional strongly-coupled $SU(N_c)$ $\mathcal{N} = 4$ super-symmetric Yang-Mills theory ($\mathcal{N} = 4$ SYM) at the large-N_c limit with a single flavor of fundamental $\mathcal{N} = 2$ hypermultiplet. This is a supersymmetric cousin of quantum chromodynamics (QCD), but its supersymmetry is broken at finite temperatures. The $\mathcal{N} = 4$ SYM sector (gluon sector) contains the gauge particles in the adjoint representation, which we call "gluons" in this Letter. The $\mathcal{N} = 2$ hypermultiplet sector (quark sector) contains particles in the fundamental representation and antifundamental representation; we call these particles "quarks" and "antiquarks," respectively. The quark (antiquark) carries a unit of positive (negative) quark charge. These particles play the role of, for example, electrons and holes in condensed matter, that is, the role of charge carriers. The interaction among these particles is mediated by the gluons; the gluons play the role of phonons, for example.

We consider the conductivity associated with the quark charge, and it is the quark-charge current that drives the quark sector out of equilibrium. NESS is realized in the following manner [8]. We set the large-N_c limit that makes the degree of freedom (DOE) of the gluon sector [which is $O(N_c^2)$] sufficiently larger than that of the quark sector [which is $O(N_c)$]. We also set the gluon sector equilibrium at a definite temperature T. The interaction between the gluon sector and the quark sector generates a dissipation in the presence of the quark current: the gluons absorb the momentum and the energy of the charge carriers. Because of the large DOE, the heat capacity of the gluon sector is sufficiently large, and the temperature of the gluon sector is well approximated as a constant. The gluon sector plays the role of heat bath, and the NESS of the quark sector is realized by putting the dissipation into the heat bath and the work of the external field in balance.

Let us specify the conditions we impose on the system. We consider a neutral system where the total quark-charge density is zero. This means that the finite current is realized by equal numbers of quarks and antiquarks flowing in opposite directions. The system works as an insulator when E and T are sufficiently small compared to the mass of the quark, but a strong enough electric field will break the insulation [9,10]. Our charge carriers are those pair created by the external field [11] in the insulation breaking. We assume that the system is steady and homogeneous. We also assume that the system has an infinitely large volume: note that we are not dealing with mesoscopic systems. We consider current-driven phenomena, and choose J (the quark-charge current density) as our control parameter. In this sense, E, the external field acting on the quark charge, is taken as a function of J. We choose the

electric field (and hence the current) to be in the x direction. We employ the natural units $c = \hbar = k_B = 1$.

Nonlinear conductivity in AdS/CFT.—The gravity dual of our microscopic theory is the so-called $D3 - D7$ system [12]. The computational technique of nonlinear conductivity has been proposed in Ref. [11] in the framework of the AdS/CFT correspondence, and we follow it. We sketch the idea of Ref. [11] below to define our notation, and one may consult Refs. [11,12] for more details. Our proposals for thermodynamic potential and critical exponents shall be given later.

The gluon sector at finite temperature is mapped to the gravity theory on a curved geometry, which is a direct product of a five-dimensional AdS-Schwarzschild black hole (AdS-BH) and S^5 [3]. The metric of the AdS-BH part is given by $ds^2 = -\frac{1}{z^2}\frac{(1-z^4/z_H^4)^2}{1+z^4/z_H^4}dt^2 + \frac{1+z^4/z_H^4}{z^2}d\vec{x}^2 + \frac{dz^2}{z^2}$, where z ($0 \leq z \leq z_H$) is the radial coordinate of the black hole geometry [13]. The AdS-BH has a horizon at $z = z_H$ and a boundary at $z = 0$. The Hawking temperature, which corresponds to the temperature of the gluon sector (hence that of the heat bath), is given by $T = \sqrt{2}/(\pi z_H)$; $\vec{x}$ and t denote the $(3 + 1)$-dimensional spacetime coordinates on which the gauge theory is defined. The metric of the S^5 part is given by $d\Omega_5^2 = d\theta^2 + \sin^2\theta d\psi^2 + \cos^2\theta d\Omega_3^2$, where $0 \leq \theta \leq \pi/2$, and $d\Omega_d$ is the volume element of the unit d-dimensional sphere. The radius of the S^5 part is taken to be 1 for simplicity. This is equivalent to choosing the 't Hooft coupling λ of the gauge theory at $\lambda = (2\pi)^2/2$.

The quark sector is mapped to a $D7$-brane [14] embedded to the above geometry. The three-dimensional part of the $D7$-brane is wrapped on the S^3 part in S^5, the radius of which is given by $\cos\theta$: the configuration of the $D7$-brane is specified by the function $\theta(z)$ [12]. We employ the probe approximation where the backreaction of the $D7$-brane to the AdS-BH is neglected. This is justified at the large-N_c limit, and is consistent with the picture of the AdS-BH as the heat bath. The behavior of $\theta(z)$ at the vicinity of the boundary is related to the current quark mass m_q [12] as $\theta(z) = m_q z + \frac{1}{2}[\langle \bar{q}q \rangle/N + m_q^3/3]z^3 + O(z^5)$. Here, $\langle \bar{q}q \rangle$ denotes the chiral condensate [15]. Throughout the analysis, we fix m_q at a designed value. There is a $U(1)$ gauge field A_μ on the $D7$-brane. E and J are related to A_x through $A_x(z, t) = -Et + \text{const} + J(2N)^{-1}z^2 + O(z^4)$, where $N = N_c/(2\pi)^2$ in our convention, and we have employed the gauge $\partial_x A_t = 0$ [11]. The dynamics of $\theta(z)$ and $A_x(z, t)$ is governed by the $D7$-brane action, $S_{D7} = \int dt d^3x dz \mathcal{L}_{D7}$, where $\mathcal{L}_{D7}$ is explicitly written as $\mathcal{L}_{D7} = -Ng_{xx}\cos^3\theta\sqrt{|g_{tt}|g_{xx}g_{zz} - g_{zz}(\dot{A}_x)^2 + |g_{tt}|(A_x')^2}$ [11]. Here, the prime (the dot) denotes the differentiation with respect to z (t); g_{tt}, g_{xx}, and g_{zz} are the components of the induced metric on the $D7$-brane, and they are equal to those of the metric of AdS-BH except for $g_{zz} = 1/z^2 + \theta'(z)^2$. If we regard z as a "time coordinate," $J = \partial \mathcal{L}_{D7}/\partial A_x'$ is a

conserved "canonical momentum," since $\mathcal{L}_{D7}$ does not contain A_x explicitly. Then it is convenient to introduce a "Routhian" $\tilde{\mathcal{L}}_{D7} = \mathcal{L}_{D7} - A'_x \partial \mathcal{L}_{D7}/\partial A'_x$ [16,17], which is given in terms of $\dot{A}_x$, J, θ, and θ': $\tilde{\mathcal{L}}_{D7} = -\sqrt{g_{zz}(g_{xx} - \dot{A}_x^2/|g_{tt}|)(N^2|g_{tt}|g_{xx}^2\cos^6\theta - J^2)}$ [11]. The Euler-Lagrange equation from $\tilde{\mathcal{L}}_{D7}$ determines $\theta(z)$ under given $E = -\dot{A}_x$ and J. The relationship between E and J is determined by requesting the on-shell $D7$-brane action to be real valued. This condition yields $\sigma = NT(e^2 + 1)^{1/4}\cos^3\theta(z_*)$, where $z_* = [\sqrt{e^2 + 1} - e]^{1/2}z_H$ and $e = 2E/(\pi\sqrt{2\lambda}T^2)$ [11]; $z = z_*$ is the location where the inside of the square root in $\tilde{\mathcal{L}}_{D7}$ touches zero [11].

We need numerical analysis to obtain $\theta(z_*)$ explicitly. The boundary conditions we employ are $\theta(z)/z|_{z=0} = m_q$ and $\theta'|_{z=z_*} = [B - \sqrt{B^2 + C^2}]/(Cz_*)$. Here $B = 3z_H^8 + 2z_H^4z_*^4 + 3z_*^8$ and $C = 3(z_*^8 - z_H^8)\tan\theta(z_*)$. The condition for $\theta'|_{z=z_*}$ comes from the equation of motion (EOM) at $z = z_*$ [5,9] with the assumption $\theta(z_*) \neq \pi/2$. Note that $\theta'|_{z=z_*}$ is given in terms of E, T, and J for given λ and N_c. After the solution $\theta(z)$ is obtained, we estimate m_q from $\theta(z)/z|_{z=0}$ as a function of E, T, and J. We choose E (under given T and J) so that m_q agrees with the designed value. Since the numerical analysis becomes unstable at $z = 0$, $z = z_*$, and at $z = z_H$, we avoid these points by introducing small cutoffs in the numerical computations.

Nonequilibrium phase transitions.—Let us fix $N_c = 40$ for numerical computation. We fix $m_q = 1$ for simplicity. The J-E characteristics at various T are shown in Fig. 1. The system exhibits NDC in the small-J region, whereas PDC is seen in the large-J region. The NDC region is smoothly connected to the PDC region for $T < T_c$, showing a crossover at point A. However, the curve for $T > T_c$
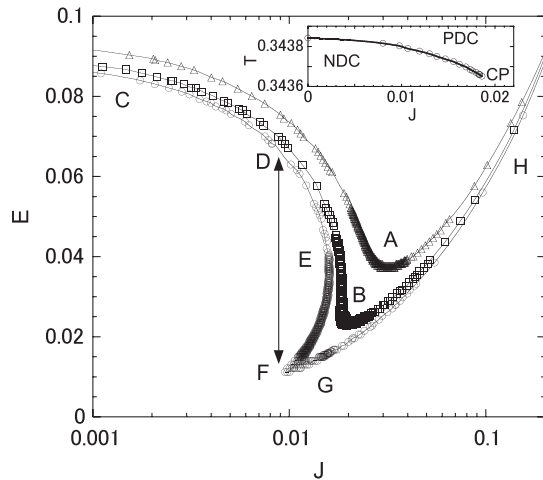

FIG. 1.   The J-E curves at $T = 3.4379 \times 10^{-1} > T_c$ (circle), $T = 3.4365 \times 10^{-1} = T_c$ (box), and $T = 3.4337 \times 10^{-1} < T_c$ (triangle). Inset: the phase diagram. *CP* denotes the critical point.

has an intermediate region (between points D and G), where three values of E are possible at a given J. This multivalued nature of E at a given J has never been obtained in earlier works. In terms of the $D7$-brane dynamics, we have three different solutions to the EOM of $\theta(z)$. If we start in the small-J region, E has to jump to the lower value at somewhere in the intermediate region, and then PDC appears. Since E (hence σ) changes discontinuously, we call it a first-order transition. The boundary between the crossover regime and the first-order regime is found at $T = 3.4365 \times 10^{-1} = T_c$. The differential resistivity $\partial E/\partial J$ diverges at $J = 1.86 \times 10^{-2} = J_c$ (indicated by B), although σ changes continuously. We call this transition at $(T, J) = (T_c, J_c)$ a second-order transition. The minimum value of E for each curve is the critical electric field for insulation breaking.

An immediate question is how to determine the transition point in the intermediate region. In equilibrium systems, the stable phase is the phase of minimum thermodynamic potential (TP), and the transition point is where the two phases share a common TP. However, the generalization of the idea of TP into nonequilibrium cases has not been completely established. One way to evaluate the NESS generalization of TP is to use the Maxwell construction [18]. However, this method works only for the pairs of conjugate variables. In our case, we need a TP as a function of J. The variable conjugate to J is $A_x|_{z=0}$ (but not E), which explicitly depends on time, and we cannot construct a time-independent TP by integrating $A_x|_{z=0}$ with respect to J: the method of Maxwell construction does not work for our purpose. Note that the Euclidean on-shell action of $D7$-brane cannot be employed as the TP in our system, since the reflection of real time is essential in nonequilibrium systems. If we insist with the Euclidean formalism, we encounter unremovable conical singularity in the gravity dual [19]. In this sense, we do not employ the Euclidean action proposed in Ref. [20]. We need a new proposal for NESS generalization of TP within the Minkowski signature.

Interestingly, we can determine the most stable phase by considering the Hamiltonian of the $D7$-brane in the gravity dual. The question is which $D7$-brane configuration is most stable among the three possible solutions. Since the dynamics of the $D7$-brane in the dual picture is governed by classical mechanics, the most stable configuration is that of the smallest Hamiltonian. We have seen that the D7-brane dynamics is governed by $\tilde{\mathcal{L}}_{D7}$. Therefore, let us construct the Hamiltonian density $\tilde{\mathcal{H}}_{D7} = \dot{A}_x \partial \tilde{\mathcal{L}}_{D7}/\partial \dot{A}_x - \tilde{\mathcal{L}}_{D7}$, which is explicitly given by $\tilde{\mathcal{H}}_{D7} = g_{xx}\sqrt{|g_{tt}g_{zz}|}\sqrt{\frac{N^2\cos^6\theta|g_{tt}|g_{xx}^2 - J^2}{|g_{tt}|g_{xx} - E^2}}$ [21]. Note that $\tilde{\mathcal{H}}_{D7}$ is regular at the horizon (where $g_{tt} = 0$) and free from the IR divergence discussed in Refs. [8,20]. The divergence at the horizon in $\tilde{\mathcal{L}}_{D7}$ is canceled by that in $\dot{A}_x \partial \tilde{\mathcal{L}}_{D7}/\partial \dot{A}_x$ within

the Legendre transformation. We propose to define the thermodynamic potential per unit 3d volume in our system by $\tilde{H}_{D7}(T, J; m_q) = \lim_{\epsilon \to 0}[\int_{\epsilon}^{z_H} dz \tilde{\mathcal{H}}_{D7} - L_{count}(\epsilon)]$, where L_{count} denotes the counterterms that renormalize the divergence at the boundary $z = 0$ (which corresponds to UV divergence in the gauge theory). L_{count} is given by $L_{count} = L_1 + L_2 - L_F + L_f$, where L_1, L_2, L_F, and L_f are explicitly given in Ref. [11,22]. Note that the relative sign between L_F and the others has to be flipped, compared to the counterterms for the action, owing to the Legendre transformation.

It is found from our numerical analysis that the configurations between F and G have the smallest $\tilde{H}_{D7}$ compared to those between E and F and those between D and E at a given J. Therefore, the transition point between NDC and PDC is D or F, as is indicated by the arrow in Fig. 1. Our system prefers the smallest dissipation under the current-controlled setup.

The next question is how to define the critical exponents. We find that the NDC and PDC phases are connected via the crossover region on the phase diagram (shown in the inset of Fig. 1): the symmetry of the system does not change through the transition. This resembles the liquid-gas transitions and the Mott insulator-to-metal transitions in equilibrium systems, whose critical points are in the same universality class of the Ising model [23]. In the liquid-gas transitions, the critical exponents β and δ are given by $\triangle \rho \propto |T - T_c|^{\beta}$ along the first-order transition line and $|\rho - \rho_c| \propto |P - P_c|^{1/\delta}$ along the $T = T_c$ line. Here, ρ and P are the density and the pressure, and ρ_c and P_c their critical values, respectively. $\triangle \rho$ is the difference of the density between the liquid phase and the gas phase. In the equilibrium Mott insulator-to-metal transitions, the critical exponents can be detected by using the conductivity instead of the density [23,24]. Therefore, let us generalize the definition of the exponent β into the nonequilibrium cases as $\triangle \sigma \propto |T - T_c|^{\beta}$, where the temperature is that of the heat bath and $\triangle \sigma$ is the difference of the conductivity between the NDC phase and the PDC phase along the first-order transition line. We regard $\triangle \sigma$ as a probe of the order parameter. The pressure of the system is not a control parameter within the present setup, but we have J instead. Let us define a new critical exponent $\tilde{\delta}$ by $|\sigma - \sigma_c| \propto |J - J_c|^{1/\tilde{\delta}}$ along the $T = T_c$ line.

The behaviors of the conductivity are plotted in Figs. 2(a) and 2(b). Critical phenomena with $\beta = 0.52 \pm 0.03$ and $\tilde{\delta} = 3.1 \pm 0.2$ are numerically found. The conductivities in the two phases and their average, along the first-order transition line, are shown in Fig. 2(c). They resemble the coexistence line and the law of rectilinear diameter in the liquid-gas transitions [25]. In Figs. 2(d) and 2(e), the behaviors of the chiral condensate are shown. The chiral condensate is more sensitive to the possible numerical errors since it is read by $\partial_z^3 \theta|_{z=0}$: we need further analysis to estimate the precise values of the exponents.
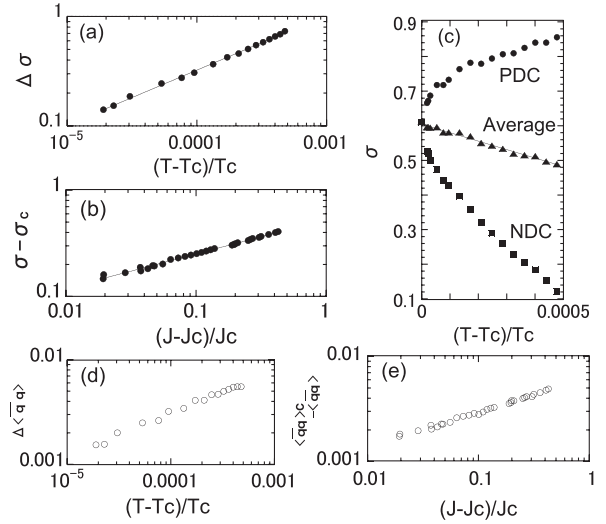

FIG. 2. Critical behaviors of various quantities. (a): $\Delta \sigma$, (b): $\sigma - \sigma_c$, (c): conductivities and the average, (d): $\Delta \langle \bar{q} q \rangle$, and (e): $\langle \bar{q} q \rangle_c - \langle \bar{q} q \rangle$.

Currently, we observe preliminary values of the exponents $\beta_{chiral} \sim 0.4$ and $\tilde{\delta}_{chiral} \sim 3$, where we have defined the exponents by using the chiral condensate instead of the conductivity.

*nakamura@ruby.scphys.kyoto-u.ac.jp
[1] J. M. Maldacena, Adv. Theor. Math. Phys. **2**, 231 (1998); , Int. J. Theor. Phys. **38**, 1113 (1999).
[2] S. S. Gubser, I. R. Klebanov, and A. M. Polyakov, Phys. Lett. B **428**, 105 (1998); E. Witten, Adv. Theor. Math. Phys. **2**, 253 (1998).
[3] E. Witten, Adv. Theor. Math. Phys. **2**, 505 (1998).
[4] M. Henkel, H. Hinrichsen, and S. Lübeck, *Non-Equilibrium Phase Transitions*. Vol. 1 (Springer-Verlag Dordrecht, 2008); M. Henkel and M. Pleimling, *Non-Equilibrium Phase Transitions*. Vol. 2 (Springer-Verlag Dordrecht, 2010).
[5] S. Nakamura, Prog. Theor. Phys. **124**, 1105 (2010).

[6] E. Schöll, *Nonlinear Spatio-Temporal Dynamics and Chaos in Semiconductors* (Cambridge University Press Cambridge, England 2001).

[7] T. Oka and H. Aoki, Lect. Notes Phys. **762**, 251 (2009).

[8] A. Karch, A. O'Bannon, and E. Thompson, J. High Energy Phys. 04 (2009) 021.

[9] T. Albash, V. G. Filev, C. V. Johnson, and A. Kundu, J. High Energy Phys. 08 (2008), 092.

[10] J. Erdmenger, R. Meyer, and J. P. Shock, J. High Energy Phys. 12 (2007) 091.

[11] A. Karch and A. O'Bannon, J. High Energy Phys. 09 (2007) 024.

[12] A. Karch and E. Katz, J. High Energy Phys. 06 (2002) 043.

[13] We have taken the string tension to be 1 for simplicity.

[14] J. Polchinski, *String Theory. Vol. 1* (Cambridge University Press, Cambridge, England, 1998) Vol. 2.

[15] The exact operator for the present model is written in Ref. [16].

[16] S. Kobayashi, D. Mateos, S. Matsuura, R. C. Myers, and R. M. Thomson, J. High Energy Phys. 02 (2007) 016.

[17] S. Nakamura, Y. Seo, S. J. Sin, and K. P. Yogendran, J. Korean Phys. Soc. **52**, 1734 (2008).

[18] O. Bergman, G. Lifschytz and M. Lippert, J. High Energy Phys. 05 (2008) 007.

[19] J. Sonner and A. G. Green, arXiv:1203.4908.

[20] M. S. Alam, V. S. Kaplunovsky, and A. Kundu, J. High Energy Phys. 04 (2012) 111.

[21] We write the Hamiltonian density in terms of E rather than $p_A = \partial \hat{\mathcal{L}}_{D7}/\partial \dot{A}_x$ for convenience of numerical estimation.

[22] A. Karch, A. O'Bannon and K. Skenderis, J. High Energy Phys. 04 (2006) 015.

[23] S. Papanikolaou, R. M. Fernandes, E. Fradkin, P. W. Phillips, J. Schmalian, and R. Sknepnek, Phys. Rev. Lett. **100**, 026408 (2008).

[24] P. Limelette, A. Georges, D. Jérome, P. Wzietek, P. Metcalf, and J. M. Honig, Science **302**, 89 (2003); F. Kagawa, K. Miyagawa, and K. Kanoda, Nature (London) **436**, 534 (2005).

[25] P. M. Chaikin and T. C. Lubensky, *Principles of Condensed Matter Physics* (Cambridge University Press, Cambridge, England, 1995), pp. 165–167.